Scholar Publishing Group
International Journal of Big Data Intelligent Technology
https://doi.org/10.38007/IJBDIT.2021.020403
ISSN 2790-0932 Vol. 2, Issue 4: 17-32

Image Processing Method for Automatic Identification of Carbon Nanotubes Based on SEM

Feigao Li*

Henan Polytechnic, Zhengzhou 450046, Henan, China

lifeigao@163.com

**corresponding author*

Keywords: Scanning Electron Microscopy, Carbon Nanotubes, Automatic Identification, Image Processing

Abstract: Carbon nanotubes are typical one-dimensional materials that can be metals or semiconductors. At present, research on SEM image processing methods is becoming more and more common, so it is particularly meaningful to use SEM to automatically identify carbon nanotubes. In this paper, a scanning electron microscope-based automatic detection method for carbon nanotubes is proposed, and a method for classifying low-dimensional nanomaterials in scanning electron microscope (SEM) images is also presented. Based on the scanning electron microscope images of nanomaterials, the surface texture of the materials was extracted by the automatic detection technology of carbon nanotubes (CNTs). The test results show that the simulation results of SEM images of 10 different materials show that the classification accuracy of the method can reach 93.75%, which proves its effectiveness in practical engineering.

1. Introduction

In recent years, great progress has been made in nanotechnology-based nanomaterials, among which carbon nanotubes (CNTs) are a representative new type of nanomaterials. As a kind of nanotechnology, nanomaterials have made great progress in recent years, among which carbon nanotubes are one of the most representative new nanomaterials. Carbon nanotubes, like graphene and fullerenes, are the same variants of carbon. Single-walled carbon nanotubes (CNTs) can be regarded as a special semi-one-dimensional tubular structure of graphene. Because the diameter of carbon nanotubes is very small and the aspect ratio is very large, there are no dangling bonds on the outer wall in the natural state, so they are very stable one-dimensional materials. Some effects specific to one-dimensional materials, such as the Coulomb blockade effect, can be observed by using carbon nanotubes. At the same time, the large specific surface area of carbon nanotubes also makes it have important applications in energy storage and catalysis.

Compared with traditional materials, carbon nanotubes have certain advantages in electrical, mechanical, thermal, optical and other aspects. With the increase of social demand and the continuous deepening of nanomaterials research, magnetic nanomaterials stand out from many nanomaterials due to their excellent magnetic properties and broad application prospects, which have attracted the attention of many scholars. At present, carbon nanotubes have certain applications in both macroscopic and microscopic fields. Taking advantage of the size and elasticity of carbon nanotubes, carbon nanotubes can be used in atomic force microscopy (AFM) and field emission devices. On the macro side, the touchscreen is a conductive film made of carbon tubes. Flexible carbon nanotubes are used to make composite materials as well as capacitors and hydrogen storage materials.

The innovation of this paper is to provide an image processing method for automatic identification of carbon nanotubes based on SEM (Scanning Electron Microscope), which is innovative and practical.

2. Related Work

As a special new material, carbon nanotubes still have many unique properties to be developed and applied to more broad fields. Many scholars have studied it. Compared with the symmetrical structure, there are many kinds of asymmetric structures of single-walled carbon nanotubes. Ghadyani G provides the first comprehensive characterization of all possible chirality. To characterize asymmetric single-walled carbon nanotubes (SWCNTs), he employed several finite element models to obtain a logical relationship between the geometry of symmetric and asymmetric configurations and their shear moduli [1]. Functionalization is a key technology to improve the dispersibility of carbon nanotubes (CNTs) in solvents and polymer matrices, which can be used to prepare multifunctional CNT-based materials. Therefore, a robust and efficient characterization method is needed to confirm that the functionalization of carbon nanotube surfaces is spatially uniform. Here, Nakajima H demonstrated high spatial resolution energy dispersive X-ray spectroscopy (EDS) imaging of functionalized single-walled carbon nanotubes (SWCNTs) in scanning electron microscopy (SEM) [2]. Carbon nanotubes (CNTs) still receive extensive attention in the field of biosensing due to their excellent properties. Mohana K V successfully fabricated fibrous carbon nanotubes (f-CNTs) on copper-molybdenum (Cu-Mo)-substituted alumina nanoparticles using chemical vapor deposition (CVD) technique at atmospheric pressure, and effectively used it as a neurotransmitter dopamine (DA) sensor [3]. Kim H S fabricated multi-walled carbon nanotubes (MWCNTs) on gold electrodes to develop a low-resistance resistive-sensing humidity sensor. He used chitosan-multi-walled carbon nanotubes to prepare nano-hybrid materials with a core-shell structure to obtain good hydrophilicity, thereby obtaining a high-response humidity sensor [4]. Hesabi M studied the adsorption behavior of atenolol molecules on pristine carbon nanotubes, boron nitride nanotubes and functionalized carbon nanotubes. He uses natural bond orbitals, non-covalent interactions and quantum theory of atoms in molecules to study hydrogen bonding, interaction energy and charge transfer between atenolol drug and nanosystems [5]. Dhore VG presented work on Fe-Co-Ni ternary catalysts with different ratios of 3%, 5%, 7% and 10%, and the deposition was carried out in the temperature range of 600℃ to 750℃ [6]. Suslova E V studied the effect of concentration, time and procedure on the surface oxidation treatment of carbon nanotubes (CNTs) and nitrogen-doped carbon nanotubes (N-CNTs) [7]. In the study of Mohammad MR, unprocessed single-walled carbon nanotubes (SWCNTs) and multi-walled carbon nanotubes (MWCNTs) were chemically treated with sulfuric acid (H_2SO_4) and

nitric acid (HNO_3) ratio (3:1) [8]. However, the shortcomings of these studies are that the model construction is not scientific enough and the data is not well prepared to adapt to more complex situations.

3. Method for Automatic Identification of Carbon Nanotubes Based on SEM

3.1. Introduction to Carbon Nanotubes

Carbon nanotubes (CNTs) are ideal one-dimensional quantum well materials due to their small size, large surface area, and high gas absorptivity, making them ideal gas sensors. There are generally considered three types of carbon: diamond, graphite and amorphous carbon. Carbon nanotubes (CNTs) have attracted much attention due to their excellent properties and potential applications [9].

(1) Molecular structure of carbon nanotubes

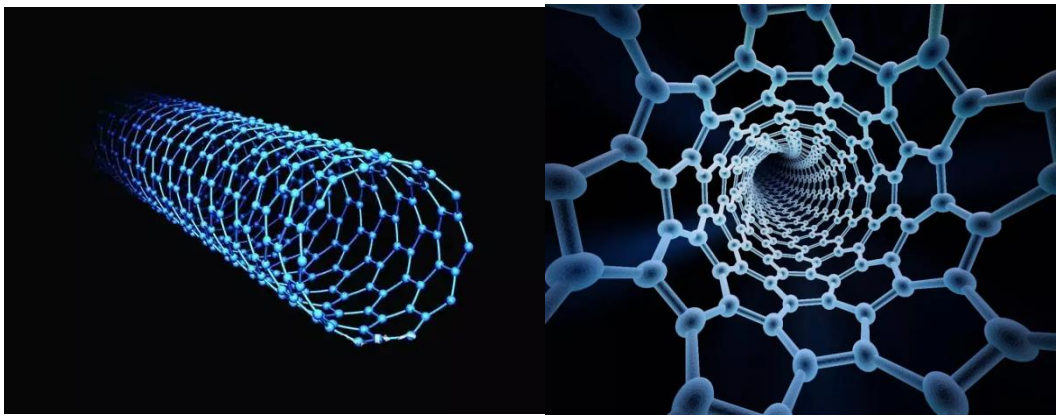

(a) (b)

Figure 1. Molecular structure of carbon nanotubes

Carbon nanotubes are seamless nanoscale tubes made of single-layer or multi-layer graphite sheets rolled around a central axis at a certain helix angle, as shown in Figure 1.

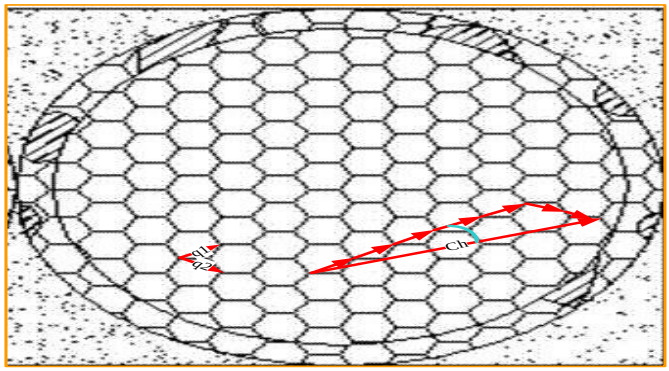

Figure 2. Schematic diagram of graphite winding to form carbon nanotubes

According to the different number of layers of carbon atoms in carbon nanotubes, carbon nanotubes can be divided into two categories: single-walled carbon nanotubes (SWNTs) and multi-walled carbon nanotubes (MWNTs). Carbon nanotubes can be thought of as entangled graphite along a chiral support. The vector design when the graphite plane is rolled into the cylinder

is shown in Figure 2 [10].

Chiral angle:

$$\theta = \arctan\left(\sqrt{3} \bullet \frac{s}{2f + s}\right) \tag{1}$$

Tube diameter:

$$d = \frac{A_0\sqrt{3\left(s^2 + s \bullet f + f^2\right)}}{\pi} \tag{2}$$

(2) Properties of carbon nanotubes

The basic structure of carbon nanotube clips is a C-C covalent bond, which forms a closed space structure on the tube axis. Figure 3 shows the properties of carbon nanotubes.

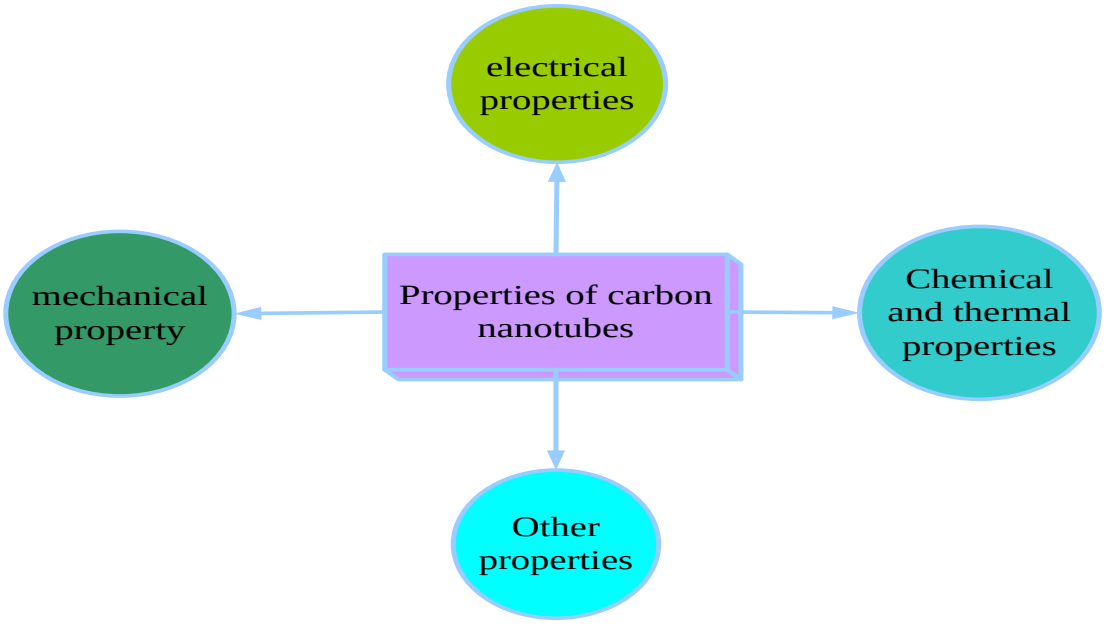

Figure 3. Properties of carbon nanotubes

1) Electrical properties

The conductivity of carbon nanotubes is related to the helical diameter of carbon nanotubes [11].

2) Mechanical properties

The C-C covalent bond gives carbon nanotubes high strength and high hardness.

3) Chemical and thermal properties

Carbon nanotubes have many structural defects, and their surface activity is higher than that of graphite paper layers, and the interaction between the defect size and the upper corners of carbon nanotubes is significantly increased.

(3) Preparation of carbon nanotubes

Since MWNTs are found in the fullerene cathode deposits generated by arc discharge, the preparation method of the present invention has the advantages of high yield, uniform particle size, less structural defects, low impurity content, low cost and convenient operation [12]. The following are several typical preparation methods (Figure 4).

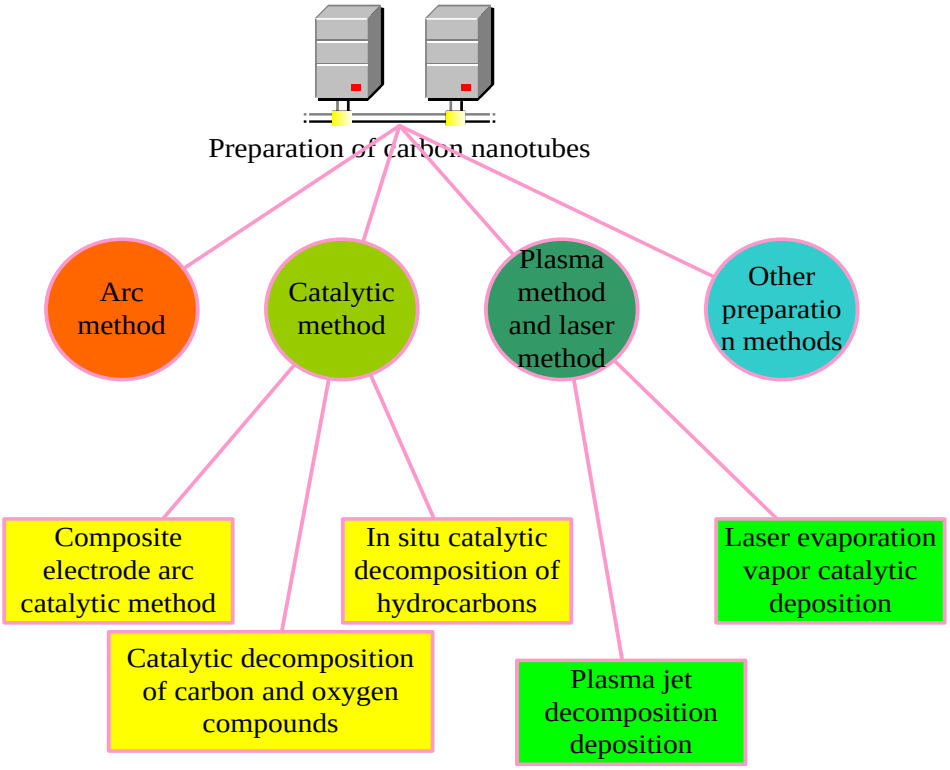

Figure 4. Preparation diagram of carbon nanotubes

(4) Application of adsorption properties of carbon nanotubes

As the nanoparticle size decreases, the adsorption efficiency of CNTs, the ratio of surface atoms to total nanoparticle atoms increases significantly, resulting in an increase in surface energy and changes in nanoparticle properties [13]. The application of adsorption performance of carbon nanotubes is shown in Figure 5.

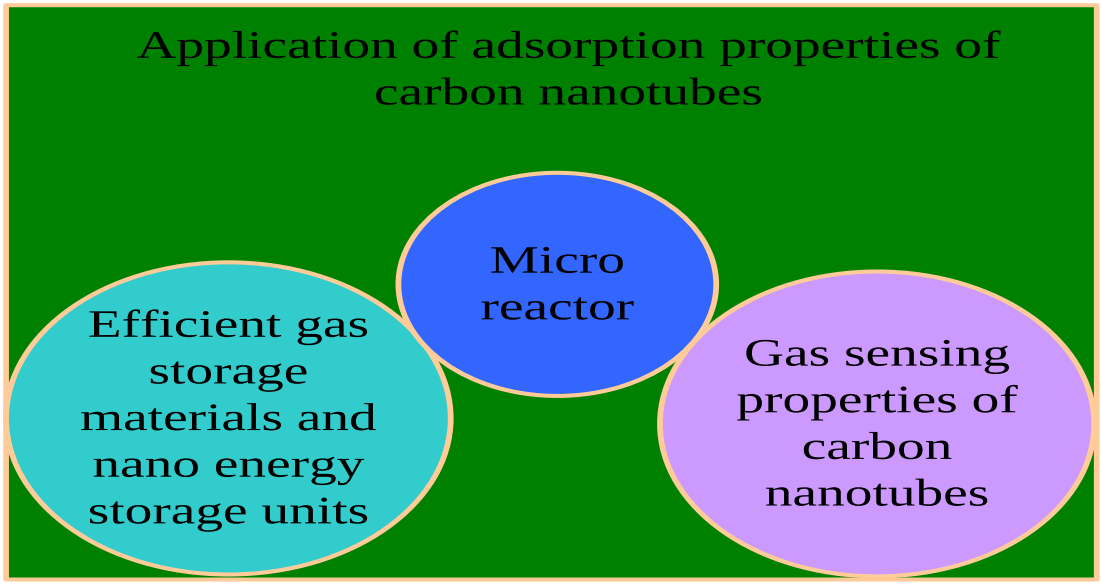

Figure 5. Application of adsorption properties of carbon nanotubes

3.2. Basics of Types

(1) Classification concept

Definition: if a set S ensures that formula (3) holds, then we call the set S a fractal set.

$$H_W(S)=H_K(S) \tag{3}$$

Among them, $H_J(S)$ is the Hartzover dimension of the set S, and $H_K(S)$ is the geometric dimension of the set S.

(2) Single fractal

Single fractal mainly refers to those fractal geometry with fixed measure or scale or things with fractal properties. After DFA processes the time series, the Hurst index is obtained, which is used to represent the self-similarity of the time series. DFA methods have been applied in many fields [14].

1) For a given sequence A(k) of length N, calculate its cumulative deviation signal B(k):

$$B(\mathrm{u})=\sum_{k=1}^{u}A(k)-\overline{A} \tag{4}$$

Among them:

$$\overline{A}=\frac{1}{M}\sum_{k=1}^{M}A(\mathrm{k}),u=1,2,3,4,\Lambda\ ,M \tag{5}$$

2) Segment the sequence $B(u)$ with equal-length regions, and divide the sequence into M_o disjoint sub-regions with length o, where $M_o=\left[\frac{M}{o}\right]$. Because the length of the sequence may not be divisible by o, sometimes there are small pieces of data that are not utilized at the end of the sequence. In order to analyze the data completely, the same data segmentation is performed on the opposite direction of the sequence, and a total of $2M_o$ small regions of equal length are obtained [15].

3) Using formula 6 to calculate the difference between the original sequence and the fitted value of each small region.

$$B_o(u)=B(u)-Q_{\mathrm{p}}(u),u=1,2,3,\Lambda\ ,M \tag{6}$$

In the formula, $Q_p(u)$ is the fitting polynomial of the vth small region.

4) Calculating the mean square error $G^2(p,o)$ of each small area after filtering out the trend.

$$G^2(p,o)=\frac{1}{o}\sum_{u=1}^{o}B_o^2((p-1)o+u),u=1,2,3,\Lambda\ ,M \tag{7}$$

$$G^2(p,o)=\frac{1}{o}\sum_{u=1}^{o}B_o^2(M_o-(o-M_o)o+u),u=M_o+1,\ M_o+2,\Lambda\ ,2M_o \tag{8}$$

5) The fluctuation signal $G(o)$ of the time series can be obtained by calculating formula 9.

$$G(o)=\sqrt{\frac{1}{2M_o}\sum_{p=1}^{2M_o}G^2(p,o)} \tag{9}$$

6) Taking the natural pair of formula 10 to obtain $\ln G(o)=Z+W\bullet\ln o$, and calculate all data points with a linear regression to obtain W, which is the Hurst exponent [16].

$$G(o)\infty o^W \tag{10}$$

(3) Multifractal theory

In this paper, multifractal theory is used to process SEM images, and multifractal parameters are extracted to quantitatively evaluate the uniformity of carbon nanotube films prepared by jet suction filtration.

In the process of analyzing data using fractal theory, many researchers have noticed a similar phenomenon. When the single fractal theory is used to describe most of the objectively existing things, the single fractal theory can only describe the global features, and lacks a more delicate characterization of the local features of the data. In the aspect of signal classification, the analysis of single fractal theory occurs in a similar phenomenon, and the fractal dimension can only describe the fractal characteristics of the signal from a single measure, and cannot fully reflect its detailed description [17].

The MFDFA method is mainly used for processing, the MFDFA method process:

1) Time series $A,\mathrm{t}=1,2,3,\Lambda\ ,T$

2) Calculating the cumulative deviation sequence B_{u}:

$$B_u=\sum_{k=1}^{u}\left(A-\overline{A}\right),\mathrm{u}=1,2,3,\Lambda\ ,T \tag{11}$$

Among them:

$$\overline{A}=\frac{1}{T}\sum_{k=1}^{T}A_k \tag{12}$$

3) Calculating the local root mean square $G(\mathrm{o},p)$:

$$\mathrm{g}(o,p)=\frac{1}{o}\sum_{u=1}^{o}\left(B_{(p-1)o+u}-B_p(u)\right)^2,p=1,2,3,\Lambda\ ,M_o \tag{13}$$

$$\mathrm{g}(o,p)=\frac{1}{o}\sum_{u=1}^{o}\left(B_{M-(p-M_o)o+u}-B_p(u)\right)^2,p=M_o+1,\ \ M_o+2,M_o+3,\Lambda\ ,2M_o \tag{14}$$

Among them, $B_p(u)$ is the R-order polynomial fitting the segment, using the least squares method, and R is generally 1, 2, 3.

4) Calculating the global root mean square $G_q(\mathrm{o})$:

$$G_q(\mathrm{o})=\begin{cases}\left(\dfrac{1}{2M_o}\sum_{p=1}^{2M_o}\mathrm{g}(o,p)^{\frac{q}{2}}\right)^{\frac{1}{q}}, q\in Randq\neq 0\\ e^{\frac{1}{4M_o}\sum_{p=1}^{2M_o}\ln g(o,p)}, q=0\end{cases} \tag{15}$$

5) According to the above formula, grouping with different q values, the q value of each group is the same, and taking different o values in the group corresponds to multiple $G^2(q;o)$. Using the following formula to obtain the W value corresponding to the q value through a single linear regression, and finally obtain multiple pairs (q,W).

$$\ln G^2(q;o)=Z+W\bullet\ln o \tag{16}$$

If A(o) is data with polyfractal properties, W and q are independent of constants, that is, the graph of the generalized Hurst exponent is a curve. If the data A(o) is a fractional time series, then W and q are related by a constant, that is, the generalized Hurst exponent graph is a horizontal straight line [18].

6) Calculating the quality index $\iota(\mathrm{q})$:

$$\iota(q)=qW(q)-1 \tag{17}$$

7) Calculating the singularity index α:

$$\alpha=\frac{\mathrm{d}\iota(q)}{dq}=W(q)+q\bullet W'(q) \tag{18}$$

Among them, $W'(q)$ is shown in formula 19.

$$W'(q_u)=\frac{W(q_u)-W(q_{u+1})}{q_u-q_{u+1}} \tag{19}$$

8) Calculating the singular spectrum $\mathrm{g}(\alpha)$:

$$\mathrm{g}(\alpha)=q\alpha-\iota(q)=q(\alpha-w(q))+1 \tag{20}$$

3.3. Neural Network Basics

1) Development of Neural Networks

The term BP neural network is actually not strict. BP refers to the algorithm for adjusting the weights and bias values of the model, that is, the back-propagation algorithm [19].

2) Classification of neural networks

The neural network has undergone several periods of development and continuous improvement. At present, there are more than 40 neural network models. On the basis of the connection mode of the neural network, the neural network can be divided into three categories.

Figure 6(a) shows the forward network model. Figure 6(b) is a self-organizing network. Figure 6(c) is the feedback network.

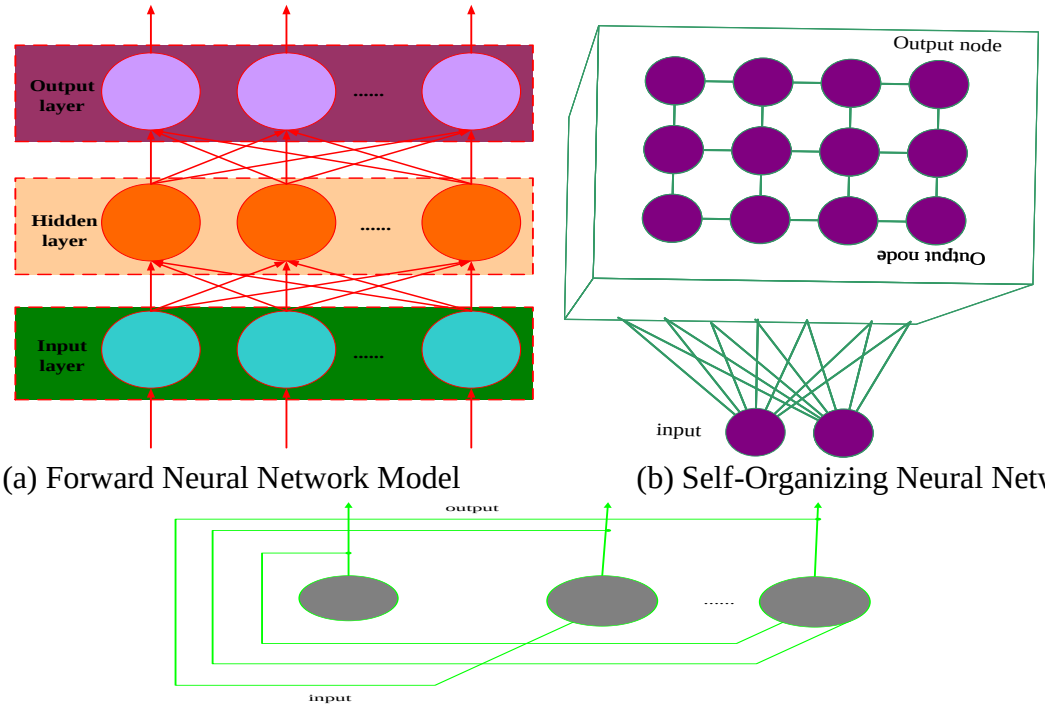

(a) Forward Neural Network Model (b) Self-Organizing Neural Network

(c) Feedback neural network

Figure 6. Neural network classification diagram structure diagram

3.4. Support Vector Machine Algorithm

(1) Theoretical basis of support vector machine

Support vector machine is a data mining technology based on statistical theory. The principle of minimum structural risk and VC dimension theory are its statistical theoretical basis. Support Vector Machine (SVM) can be regarded as a neural network with hidden layers, and SVM is explained from the perspective of neural network, as shown in Figure 7 [20].

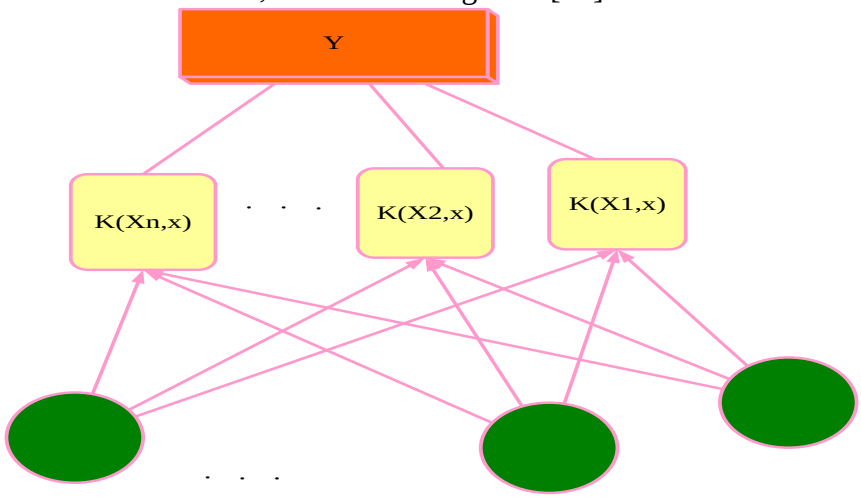

Figure 7. Schematic diagram of the structure of the support vector machine

(2) The basic idea of support vector machine
The basic idea of SVM is shown in Figure 8.
(3) Kernel function
The most studied kernel functions include:
1) Polynomial machine with kernel function

$$D(h,h_i)=(h\bullet h_i+1)^r \tag{21}$$

Among them, r is the order of the polynomial kernel.
2) Radial basis function machine with kernel function

$$D(h,h_i)=\exp\left(\frac{-1}{\delta^2(h-h_i)^2}\right) \tag{22}$$

Among them, δ is the bandwidth of the radial basis function kernel.
3) Two-layer neural network machine with kernel function

$$D(h,h_i)=F[(h\bullet h_i)]=\frac{1}{1+\exp(v(h\bullet h_i)-b)} \tag{23}$$

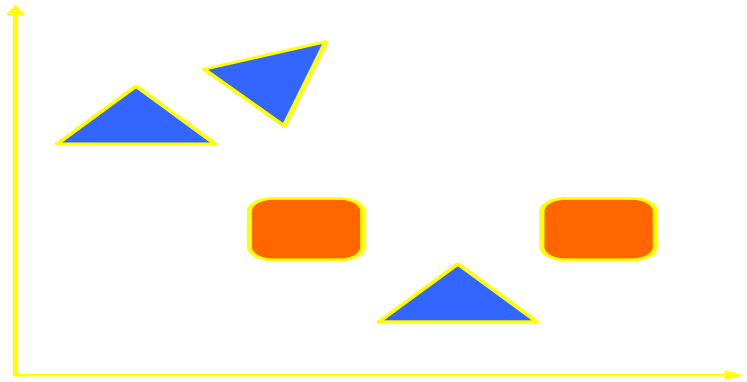

(a)

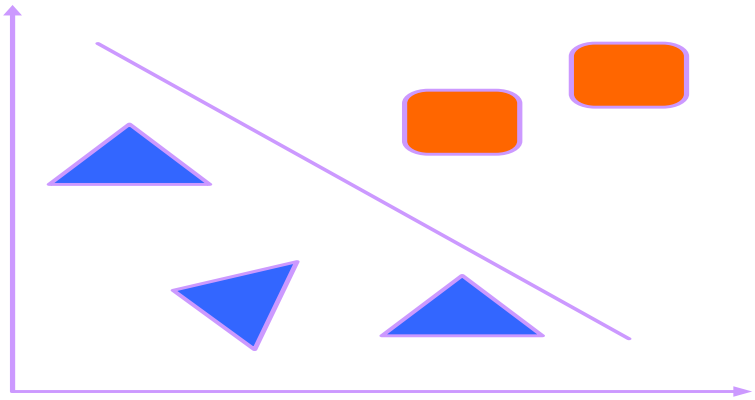

(b)

Figure 8. Basic idea of SVM

Among them, v and b are the parameters of the F-shaped function $F[(h \bullet h_i)]$ satisfying the inequality $b \geq v$. The kernel functions shown in Table 1 [21].

Table 1. Kernel functions

RBF kernel function	$D(X, X') = EXP(-\gamma \|X - X'\|^2)$
Linear kernel function	$D(X, X') = X \bullet X'$
Polynomial kernel function	$D(X, X') = (X \bullet X' + 1)^k$
Sigmoid kernel function	$D(X, X') = \tanh(\alpha < X, X' > + R)$

4. SEM-based Experiments on Carbon Nanotubes

SEM is also often used to characterize carbon nanotubes. Due to the simple sample preparation, fast image capture and very high characterization efficiency, SEM can be used for large-scale characterization and is currently the most commonly used method for topographic characterization. Since carbon nanotubes with different conductivity have different effects on the surface potential, SEM can distinguish the conductivity types of carbon nanotubes. If the contact barrier between carbon nanotubes and metal is used to image, the band gap distribution information can also be obtained. The diameter of carbon nanotubes is much smaller than the wavelength of visible light, and Rayleigh scattering occurs under illumination. The density of states of carbon nanotubes at the van Hove singularity is very large. When the energy of the incident light is equal to the energy difference corresponding to the van Hove singularity, resonant Rayleigh scattering will occur, and the position of the van Hove singularity can be known from the position of the resonance peak [22].

4.1. Specific Values of Texture Parameters

In this work, the SEM equipment provided SEM images of 10 low-dimensional nanomaterials. The class labels are registered as S-1, S-2, ... S-10 from left to right and top to bottom, 10 sample images were selected for the same nanomaterial, and a total of 10x10=100 sample images were tested.

In this paper, the DB1 function is selected to decompose the SEM images of ultrafine materials with three-layer wavelet packets, and the Gaussian radial basis kernel function and support vector machine are used to construct the classifier. Table 2 lists some structural parameters and SEM images extracted from 10 nanomaterials. It can be seen from Table 2 that the texture distribution parameters of different types of nanomaterials are quite different, which can quantitatively characterize different types of nanomaterials.

Table 2. Specific values of texture parameters

Nanomaterial category label	Band subgraph						
	1		2		...	64	
	mean value	variance	mean value	variance	...	mean value1	variance
S-1	103.4	9.59	61.66	9.001	...	2.698	3.114
S-2	115.9	10.44	30.12	8,821	...	1.507	1.698
S-3	113.2	10.23	30.99	8.091	...	1.331	2.045
S-4	58.1	9.14	31.04	7.721	...	1.609	2.321
S-5	93.9	9.57	44.01	8.309	...	2.009	2.913
S-6	115.3	10.53	33.55	8.951	...	0.798	0.942
S-7	115.2	9.89	14.99	7.699	...	1.081	1.332
S-8	163.3	12.02	19.71	7.786	...	1.276	1.795
S-9	150.1	10.82	8.92	6.617	...	0.624	0.726
S-10	108.4	10.72	29.87	8.331	...	2.462	3.471

4.2. Specific Classification Results of 10 Types of Nanomaterials

Table 3. 10 Specific classification results of nanomaterials

Nanomaterial category label	Statistics of classification number									
	S-1	S-2	S-3	S-4	S-5	S-6	S-7	S-8	S-9	S-10
S-1	15									
S-2		10	(4)							
S-3			15							
S-4				14	(1)					
S-5					15					
S-6						15				
S-7							15			
S-8								15		
S-9									15	
S-10										15

It can be seen from Table 3 that the method proposed in this paper has high classification accuracy. Through calculation, the classification accuracy is 93.75%, which fully meets the requirements of general technology. However, it can also be found that the classification accuracy of some nanomaterials is relatively low, especially the high classification error rate of S-2. The reason is that the content of SEM images of these nanomaterials is very chaotic, and their texture structures have large spatial differences and irregularities.

4.3. Secondary Electron Images of Carbon Nanotubes on Insulating Substrates

The carbon nanotube images at high voltage are noticeably finer. We made statistics on the width

of carbon nanotube images at high and low voltages, as shown in Figure 9. The average width of carbon nanotubes is 57.44 nm under the accelerating voltage of 1 kV and 22.65 nm under the accelerating voltage of 10 kV, that is, the spatial resolution of the image is doubled under the high voltage.

As can be seen from Figure 9, the secondary electron emission coefficient deviates from 1 more significantly at low voltages. We photographed at the same dwell time at both voltages, so the lower voltage is more charged, which provides electron tunneling to a wider range of substrate surfaces, resulting in a wider image.

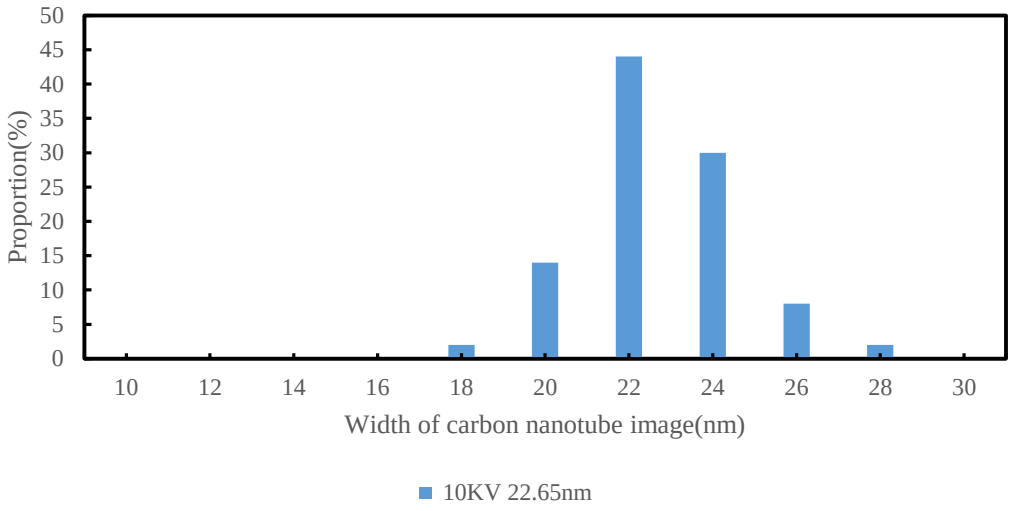

(a)

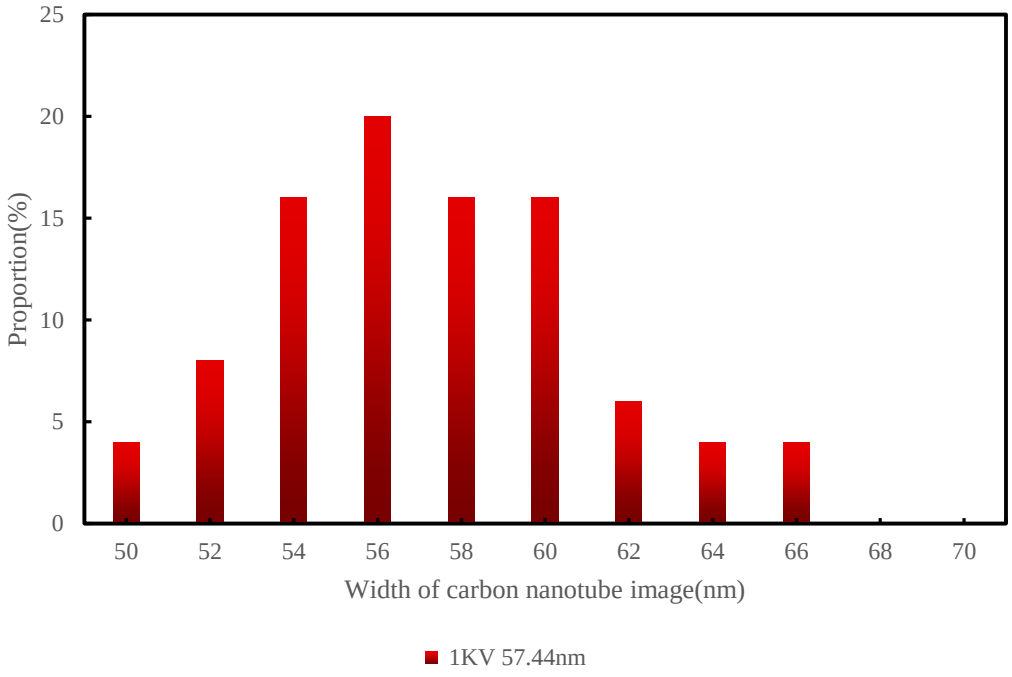

(b)

Figure 9. Width statistics of carbon nanotube images at high and low voltage on quartz substrates

5. Discussion

SEM has obvious efficiency advantages in material morphology characterization and electrical conductivity characterization, and has great application potential in large-scale rapid non-destructive characterization. In terms of carbon nanotube characterization, we studied the principle of SEM characterization of carbon nanotubes, and how to distinguish two conductivity types of carbon nanotubes under various imaging conditions.

The depletion regions of carbon nanotubes can also be imaged under SEM, including Schottky junctions and p-n junctions. The depletion regions of carbon nanotubes are bright lines at high and low accelerating voltages, and it is easier to define the length of depletion regions at high accelerating voltages due to the existence of contrast inversion.

In terms of SEM characterization of carbon nanotubes, currently only the characterization of the band gap distribution can be achieved, but the chirality identification has not yet been achieved. If SEM can be used in chiral recognition, it will greatly improve the speed of related research and applications.

6. Conclusion

This paper proposes a detection method for low-dimensional nanomaterials, which uses texture analysis theory to automatically classify and identify low-dimensional nanomaterials. It has good classification accuracy and overcomes the limitations of traditional methods and existing manual detection methods based on researchers' knowledge and experience. The results show that this is an effective attempt to apply texture analysis theory to the field of material analysis. Due to the limitation of experimental conditions, the classification of materials is relatively low, so it is necessary to further consider the SEM image database with more material categories, and consider how to extract the morphological features of materials more effectively, and improve the classification accuracy and calculation speed.

Funding

This article is not supported by any foundation.

Data Availability

Data sharing is not applicable to this article as no new data were created or analysed in this study.

Conflict of Interest

The author states that this article has no conflict of interest.

References

[1] Ghadyani G , Soufeiani L , Ochsner A . Angle dependence of the shear behaviour of asymmetric carbon nanotubes. Materials & Design, 2017, 116(feb.):136-143.

[2] Nakajima H , Morimoto T , Zhou Y , Kobashi K , Okazaki T . Nonuniform functional group distribution of carbon nanotubes studied by energy dispersive X-ray spectrometry imaging in SEM. Nanoscale, 2019, 11(44):21487-21492. https://doi.org/10.1039/C9NR07619K

[3] Mohana K V , Somanathan T , Manikandan E , Kumar T K , Uvarajan S . Neurotransmitter Dopamine Enhanced Sensing Detection Using Fibre-Like Carbon Nanotubes by Chemical Vapor Deposition Technique. J Nanosci Nanotechnol, 2018, 18(8):5380-5389. https://doi.org/10.1166/jnn.2018.15425

[4] Kim H S , Kim J H , Park S Y , Carbon nanotubes immobilized on gold electrode as an electrochemical humidity sensor. Sensors and Actuators, 2019, 300(Dec.):127049.1-127049.8. https://doi.org/10.1016/j.snb.2019.127049

[5] Hesabi M , Ghasemi G . A CAM-B3LYP DFT Investigation of Atenolol Adsorption on the Surface of Boron Nitride and Carbon Nanotubes and Effect of Surface Carboxylic Groups. Russian Journal of Physical Chemistry A, 2020, 94(8):1678-1693.

[6] Dhore V G , Rathod W S , Patil K N . Synthesis and Characterization of High Yield Multiwalled Carbon Nanotubes by Ternary Catalyst. Materials Today Proceedings, 2018, 5(2):3432–3437. https://doi.org/10.1016/j.matpr.2017.11.589

[7] Suslova E V , Savilov S V , Egorov A V , Lunin V V . Activation of the Surface of Carbon and Nitrogen-Doped Carbon Nanotubes by Calcium Nitrate: Catalytic Properties of Cobalt Supported Catalysts of the Fischer–Tropsch Process Based on Them. Kinetics and Catalysis, 2019, 60(1):87-95. https://doi.org/10.1134/S0023158419010129

[8] Mohammad M R , Ahmed D S , Mohammed M . Synthesis of Ag-doped TiO2 nanoparticles coated with carbon nanotubes by the sol–gel method and their antibacterial activities. Journal of Sol-Gel Science and Technology, 2019, 90(3):1-12. https://doi.org/10.1007/s10971-019-04973-w

[9] Karim-Nezhad G , Sarkary A , Khorablou Z , Dorraji P S . Electrochemical Analysis of Tryptophan using a Nanostructuring Electrode with Multi-walled Carbon Nanotubes and Cetyltrimethylammonium bromide Nanocomposite. Journal of Nanostructures, 2018, 8(3):266-275.

[10] L B é ja r, Huape E , Medina A , Mej ú A A , Alfonso I . Study by SEM of Carbon Nanotubes Deposited by CVD Using Al 2 O 3 and TiO 2 as Catalysts. Microscopy and Microanalysis, 2019, 25(S2):2384-2385. https://doi.org/10.1017/S1431927619012650

[11] Tingkai, Zhao, Xianglin, Coral-like amorphous carbon nanotubes synthesized by a modified arc discharge. Fullerenes, Nanotubes and Carbon Nanostructures, 2017, 25(6):359-362.

[12] Kord B , Jamshidi M , Hosseinihashemi S K . Effect of Multi-Walled Carbon Nanotubes on Viscoelastic Properties of PP/Reed Flour Composites. Journal of Polymers & the Environment, 2017, 25(4):1313-1320. https://doi.org/10.1007/s10924-016-0909-x

[13] Karimidost S , Moniri E , Miralinaghi M . Thermodynamic and kinetic studies sorption of 5-fluorouracil onto single walled carbon nanotubes modified by chitosan. Korean Journal of Chemical Engineering, 2019, 36(7):1115-1123. https://doi.org/10.1007/s11814-019-0292-0

[14] Devrim Y , Arica E D . Multi-walled carbon nanotubes decorated by platinum catalyst for high temperature PEM fuel cell. International Journal of Hydrogen Energy, 2019, 44(34):18951-18966.

[15]Anandhi, C, M, Enhanced Biocompatibility of Multi-walled Carbon Nanotubes by Surface Modification: Future Perspectives for Drug Delivery System.. AIP Conference Proceedings, 2017, 1832(1):1-3. https://doi.org/10.1063/1.4980381

[16] Belgamwar S U , Pingale A D , Sharma N N . Investigation on electrical properties of Cu matrix composite reinforced by multi-walled carbon nanotubes. Materials Today: Proceedings, 2019, 18(7):3201-3208. https://doi.org/10.1016/j.matpr.2019.07.196

[17] Afsharpour M , Dini Z . One-Pot Functionalization of Carbon Nanotubes by WO 3 /MoO 3

Nanoparticles as Oxidative Desulfurization Catalysts. Fullerenes Nanotubes and Carbon Nanostructures, 2019, 27(3):198-205.

[18] Li X , Zhang Y , Chen S . Enhancement of CO_2 Desorption from Reinforced 2-(2-Aminoethylamine) Ethanol Aqueous Solution by Multi-walled Carbon Nanotubes. Energy & fuels, 2019, 33(JUL.):6577-6584.

[19] Paran S , Sahraeian R , Naderi G , Nonlinear elastoplastic behavior induced by multiwalled carbon nanotubes in the compatibilized low density polyethylene/poly(methyl hydrogen siloxane)-grafted perlite nanocomposites. Mechanics of materials, 2019, 136(SEP.):103066.1-103066.10.

[20] He B . Rapid Detection of Nitrofuran and Its Metabolites by Using Carboxylic Multi-walled Carbon Nanotubes Modified Glassy Carbon Electrode. International Journal of Electrochemical Science, 2018, 13(5):4171-4181. https://doi.org/10.20964/2018.05.50

[21] Javadi A H , Mirdamadi S , Shakhesi S . Process optimization and microstructural analysis of aluminum based composite reinforced by multi‐walled carbon nanotubes with various aspect ratios. Materialwissenschaft und Werkstofftechnik, 2017, 48(7):719-725. https://doi.org/10.1002/mawe.201600495

[22] Patel S C , Alam O , Zhang D , Layer-by-layer, ultrasonic spray assembled 2D and 3D chemically crosslinked carbon nanotubes and graphene. Journal of Materials Research, 2017, 32(2):370-382. https://doi.org/10.1557/jmr.2016.472